Chapter 12

Preparation of Blue TiO_2 for Visible-Light-Driven Photocatalysis

Jianmin Yu, Chau Thi Kim Nguyen and Hyoyoung Lee

Additional information is available at the end of the chapter

http://dx.doi.org/10.5772/intechopen.73059

Abstract

Titanium dioxide (TiO_2), which is regarded as a semiconductor photocatalyst, has drawn attention in the applications of photocatalysis, including hydrogen evolution reaction, carbon dioxide reduction, pollutant degradation, and biocatalytic or dye-sensitized solar cells due to its low toxicity, superior photocatalytic activity, and good chemical stability. However, there are still some disadvantages such as too large energy bandgap (~3.34 eV and ~3.01 eV for anatase and rutile phases, respectively) in the absorbance of all ranges of lights, which limits the photoelectrochemical performance of TiO_2. Herein, we like to introduce photocatalytic blue TiO_2 that is obtained by the reduction of TiO_2. The blue TiO_2 consists of Ti^{3+} state with high oxygen defect density that can absorb the visible and infrared as well as ultraviolet light due to its low energy bandgap, leading to enhance a photocatalytic activity. This chapter covers the structure and properties of blue TiO_2, its possible applications in visible-light-driven photocatalysis, and mainly various synthetic methods even including phase-selective room-temperature solution process under atmospheric pressure.

Keywords: blue titanium dioxide, black titanium, synthesis method, photocatalysis, visible light

1. Introduction

TiO_2 is an extraordinarily versatile material. In 1964, Kato et al. used a TiO_2 suspension for the photocatalytic oxidation of tetralin (1,2,3,4-tetrahydronaphthalene) [1]. In 1972, the "Honda-Fujishima Effect" first described by Fujishima and Honda intensively promoted the photocatalytic field [2]. This discovery led to a new application of TiO_2 in water splitting using solar energy as the driving force of the process as well as solar energy conversion.

To date, TiO_2 nanomaterials have attracted the interest of many scientists. The focus is to modify TiO_2 structural properties or to combine supportive materials to demonstrate that TiO_2 nanomaterials are excellent photocatalysts, which can be used as dopants in novel metal-TiO_2 systems such as Pt-doped TiO_2 [3], Au-doped TiO_2, or graphene/TiO_2/carbon dot composites developed as visible light photocatalysts [3, 4].

In this chapter, we focus on blue TiO_2 as a visible-light-driven photocatalyst and its preparation methods. The blue TiO_2 nanomaterial contains Ti^{3+} with an abundant oxygen vacancy, which can absorb visible and infrared light as well as UV light, producing more electrons and holes and also facilitating better electrical conductivity than pristine TiO_2 [5]. In the future, we would like to further address the beneficial applications in clean energy storage media and protecting the environment, including the hydrogen evolution reaction, carbon dioxide reduction, and degradation of pollutants by using noble blue TiO_2 under visible light.

2. General structure and properties of TiO_2

TiO_2 belongs to the transition metal oxide family. There are four different polymorphs of TiO_2 found in nature such as anatase (tetragonal), rutile (tetragonal), brookite (orthorhombic), and TiO_2 (B) (monoclinic) [6], the most important of which are anatase and rutile. With calcination at high temperatures exceeding ~600°C, the brookite and anatase polymorphs will transform into the thermodynamically stable rutile polymorph [5].

The tetragonal anatase bulk unit cell has dimensions of a = b = 0.3733 nm and c = 0.9370 nm, and the rutile bulk unit cell has dimensions of a = b = 0.4584 nm, and c = 0.2953 nm (**Table 1**). In both structures, the octahedral distortions create the basic building units [7, 8]. The lengths and angles of octahedral coordinated Ti atoms, therefore, dictate stacking in both structures, as shown in **Figure 1**.

3. The advanced structure and properties of blue TiO_2

Zhang et al. [9] discovered that the color and crystalline phase of white P_{25} (70% anatase and 30% rutile) changed into blue color by the treatment of lithium in an ethylenediamine (Li-EDA) solution, which is the first achievement in making blue TiO_2 under atmospheric

Properties	Crystalline forms		
	Anatase	Rutile	Brookite
Crystalline structure	Tetragonal	Tetragonal	Rhombohedral
Lattice constants (nm)	$a = b = 0.3733$ $c = 0.9370$	$a = b = 0.4584$ $c = 0.2953$	$a = 0.5436$ $b = 0.9166$ $c = 0.5135$
Bravais lattice	Simple, Body centred	Simple, body centred	Simple
Density (g/cm^{-3})	3.83	4.24	4.17
Melting point (°C)	Turning into rutile	1870	Turning into rutile
Boiling point (°C)	2927[a]	–	–
Band gap (eV)	3.2	3.0	–
Refractive index (n_g)	2.5688	2.9467	2.8090
Standard heat capacity, $C^o p$	55.52	55.60	–
Dielectric constant	55	110–117	78

[a] Pressure at pO_2 is 101.325 KPa.

Table 1. Crystal structure data for TiO_2 Copyright (2014), Elsevier [15].

http://dx.doi.org/10.5772/intechopen.73059

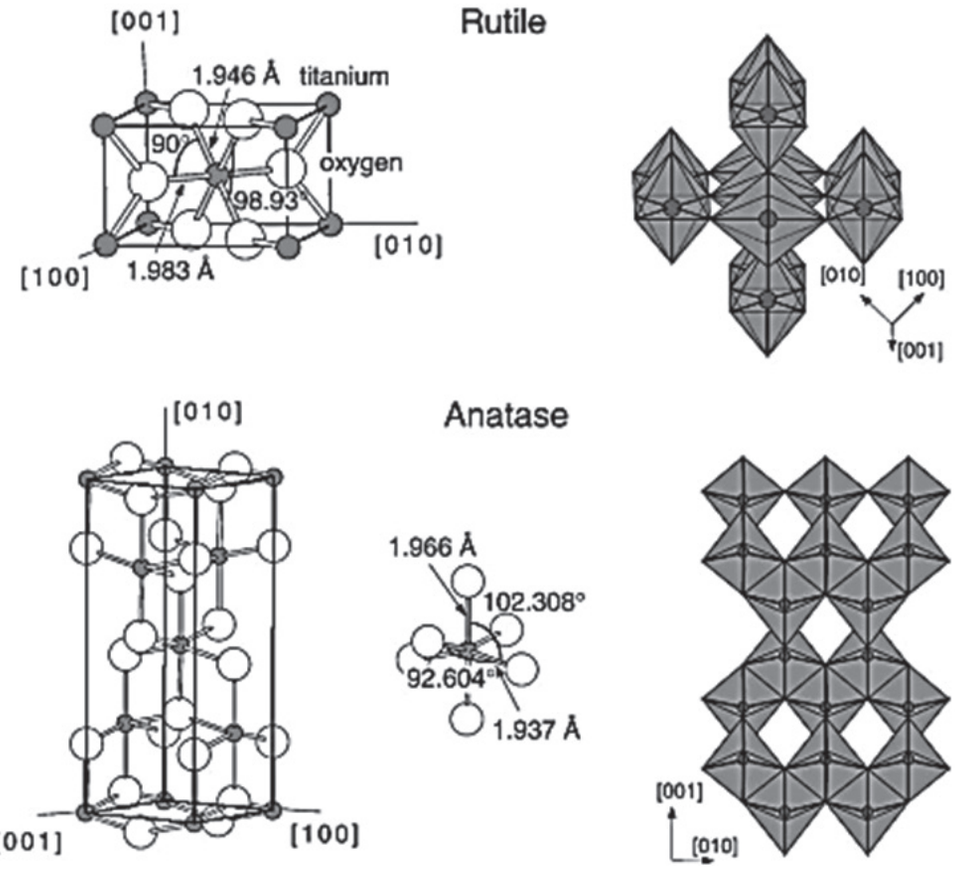

Figure 1. Bulk structures of anatase and rutile TiO_2. Copyright (2003), Elsevier [18].

pressure at room temperature in solution and also the phase-selective reduction between anatase and rutile TiO_2 phases. They showed that the white anatase TiO_2 phase was not changed, while the rutile TiO_2 phase changed into black color. In the case of P_{25} TiO_2, the blue colored TiO_2 appeared as a result of the combination of white and black colors (**Figure 2**) [9].

The unit cell parameters and nanocrystalline size profiles of white P_{25} and blue TiO_2 are shown in **Table 2**. These results show that a slight change occurred along the a and b directions, but there was significant expansion in the c direction, and as a result, the unit cell volume expanded significantly as well [10].

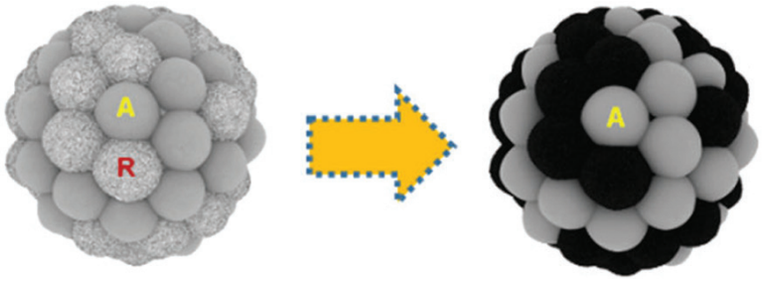

Figure 2. Schematics of TiO_2 (white P_{25}) (left) and blue TiO_2 crystals (right). The black color corresponds to the visual color of the reduced rutile TiO_2. Copyright (2016), Royal Society of Chemistry [9].

samples	cell parameter a, b/Å ($a = b$)	cell parameter c/Å	cell volume/ Å^3	crystalline size (nm)
white TiO_2	4.612 30	2.952 47	62.8088	8.774
blue TiO_2	4.611 07	2.971 47	63.1793	7.650

Table 2. Unit cell parameters of TiO_2 (white P_{25}) and blue TiO_2 Copyright (2014), American Chemical Society [10].

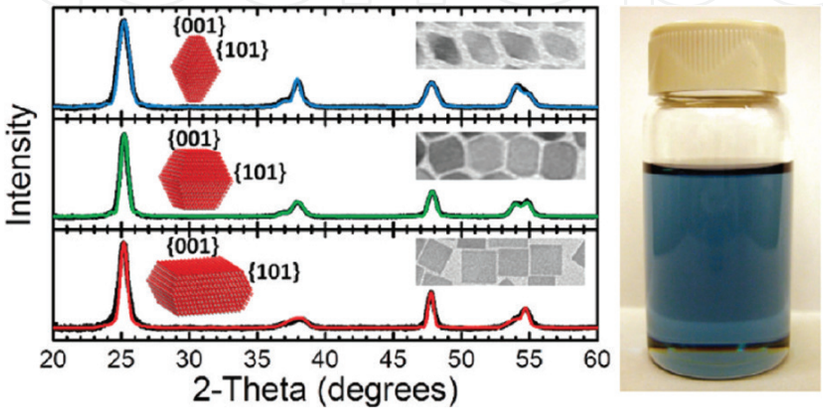

Figure 3. XRD patterns of different shapes. Experimental (thick black lines) and simulated (thin colored lines) plots for TiO_2 nanocrystals. The insets showed accurate percentages of the {001} and {101} facets of atomistic models. Copyright (2012), American Chemical Society [12].

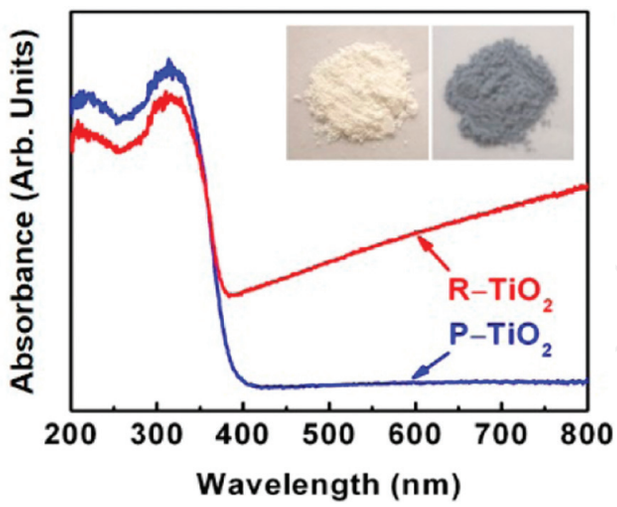

Figure 4. Color change of white P_{25} (left) to blue TiO_2 (right) and UV-vis absorption spectra of pristine TiO_2 (P-TiO_2) and reduced anatase TiO_2 (R-TiO_2). Copyright (2017), American Chemical Society [14].

Recent publications showed that the morphology of TiO_2 materials resulted in differences of the enhanced photocatalytic activity for the production of hydrogen between the {101} and {001} facets of anatase tetragonal bipyramidal nanocrystals [11–13]. Based on the XRD simulation,

the length and width of the peaks were calculated to confirm the percentages of the {101} and {001} facets (**Figure 3**). Their research well defined the optimum nanosize as well as the shape of TiO_2 crystals, suggesting that the {101} facets are more photocatalytically active than the {001} facets for the evolution of H_2 (up to 2.1 mmol h^{-1} g^{-1}) under simulated solar illumination, while the blue coloration results from oxygen vacancies in the TiO_2 lattice [12].

The blue TiO_2 has excellent absorption over a much wider spectral range than white TiO_2 due to the excitation of conduction band electrons. Therefore, it should exhibit much better photocatalytic activity under visible light or the full spectrum of solar irradiation (**Figure 4**) [9, 14].

4. Electronic properties of blue TiO_2 in photocatalysis

Semiconductor materials, TiO_2 in particular, are widely used in the applications of photocatalysis. As shown in **Figure 5**, the reduction potential of photogenerated electrons is defined by the energy level at the bottom of the conduction band (CB), while the oxidizing ability is the energy level at the top of the valence band (VB). Because the CB energy level of TiO_2 is higher than the reduction potential levels of NHE references, semiconductors as well as TiO_2 nanomaterials can be used as a catalyst for hydrogen evolution, CO_2 conversion, or pollutant degradation [15].

Photocatalytic reactions occur as a material interacts with light, which provide higher energy than the bandgap of the semiconductor to create reactive oxidizing species, leading to the photocatalytic transformation of a compound.

The basics of the photocatalytic process can be summarized as follows:

(1) TiO_2 absorption of photons with sufficient energy and generation of electron-hole pairs.

(2) Separation and transport of electron-hole pairs with electrons excited from the valence band (VB) to CB.

(3) Chemical reaction on the surface-active sites with charge carriers.

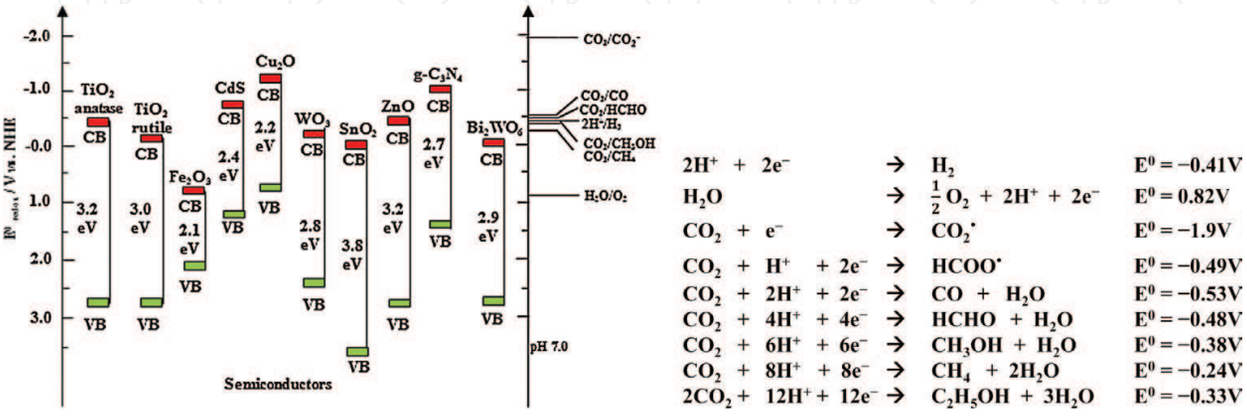

Figure 5. Bandgap of TiO_2 and some photocatalysts with respect to the redox potential (vs. NHE) values of different chemical species measured at a pH of 7. Copyright (2014), Elsevier [11, 15, 16].

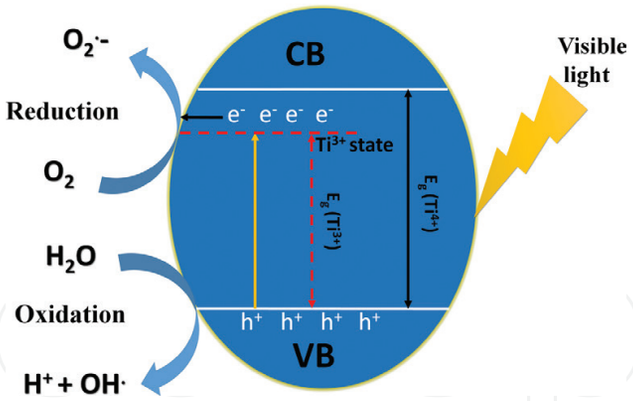

Figure 6. Schematic diagram of Ti^{3+} self-doped TiO_2 mechanism for visible light photocatalysis.

Meanwhile, electron-hole recombination is also possible depending on the competition between these processes.

Blue TiO_2 nanomaterials can overcome the limitations to enhance the photocatalytic performance due to the formation of oxygen vacancies (supports many free carriers charges). The oxygen vacancy is a positive charge. Then, Ti^{3+} from the center shifts away from the oxygen vacancy position, leading to an advanced sublevel electric state and excellently trapped holes, preventing the recombination of electrons and holes, even with the lower energy bandgap irradiation (~2.7 eV) compared to P_{25} (3.2 eV). Blue TiO_2 could generate electrons in the wide open region of irradiation such as solar light, which contains most visible and infrared wavelengths as well as UV light [17, 19] (**Figure 6**).

5. Synthesis of blue TiO_2 nanomaterials for photocatalysis

5.1. Hydrogenation synthesis

H_2 is the most common reagent used for the hydrogenation of TiO_2, which can react with the lattice oxygen, leading to the formation of abundant oxygen vacancies and Ti^{3+} in TiO_2 due to its facile activation by thermal or electromagnetic energy [4, 19]. The annealing time changes with the annealing temperature, where the blue color was maintained up to a longer time at 500°C. It readily changed to pale gray at 600°C due to the high concentration of Ti^{3+} in the bulk at the early stage of hydrogenation, which may absorb oxygen molecules and lead to O^- as a major species on the surface after prolonged hydrogenation (**Figure 7**) [20, 21]. In addition, hydrogenation processes require harsh synthetic conditions and/or a dangerous production process [4, 10, 19, 21–25]. Therefore, H_2 is introduced using different reducing agents such as $NaBH_4$ and TiH_2 [4, 26, 27] instead of an external dose of hydrogen gas. TiH_2 as a solid solution of hydrogen in Ti and P_{25} was mixed and sealed in a quartz tube and calcined at 450°C for 10 h. After discarding most of the unreacted TiH_2 sediments, HCl and H_2O_2 solutions were then introduced to completely remove the residual TiH_2, during which the TiH_2 dissolved and a yellow solution was formed. After centrifugation and thorough

http://dx.doi.org/10.5772/intechopen.73059

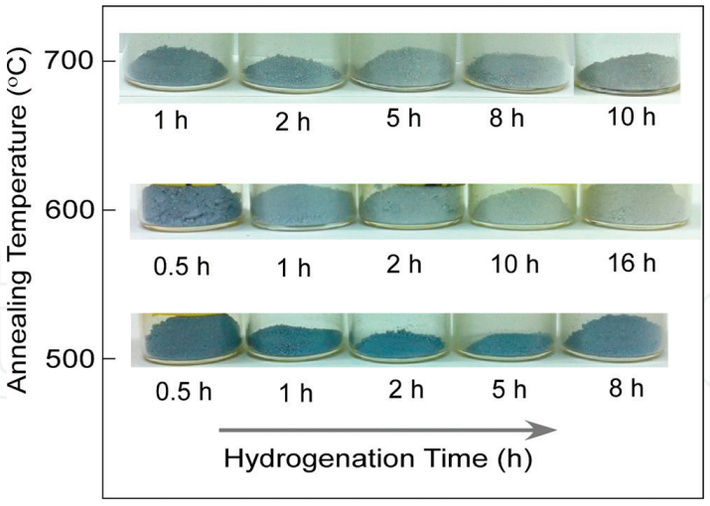

Figure 7. Photograph of H-aTiO_2 samples prepared with a H_2 gas flow at temperatures of 500–700°C. Gradual changes in color from blue to gray to a different degree are observed, depending on annealing temperatures and annealing time. Copyright (2013) American Chemical Society [21].

washing, TiH_2 was completely removed, and a well-crystallized bluish sample (TiO_{2-x}: H) was obtained [4]. Qiu et al. found that the TiO_{2-x}: H can efficiently enhance the visible- and infrared-light absorption and improve photocatalytic degradation of methyl orange (MO) and hydrogen production via water splitting by H doped into the well-crystallized lattice, which means that might be localized states in the bandgap was offered and has a relatively low recombination rate of electrons and holes. Moreover, we should note that the low concentration of hydrogen atoms in hydrogenated titania was found to be a unfavorable factor affecting the photocatalytic activity [21].

5.2. Hydro(solvo)thermal method

Hydrothermal and solvothermal methods have received some attention due to their simple and low-cost production routes and are suitable for large-scale production [28, 29]. Zhu et al. reported the synthesis of novel blue colored TiO_2 with abundant defects through a one-step solvothermal method using $TiCl_3$ and TiF_4 as precursors. The introduction of Ti^{4+} in the reaction system inhibits the oxidation of Ti^{3+} during the solvothermal treatment.

$$Ti^{3+} + \text{oxygen species} \rightleftarrows Ti^{4+} \quad (1)$$

This process is governed by the Le Chatelier's principle. The oxygen vacancy formation dominantly resulting from Ti^{3+} will not be completely oxidized during the solvothermal process. Moreover, leaving behind a high concentration of bulk Ti^{3+} defects is very favorable for visible light photocatalytic reactions [29]. In addition, Fang et al. synthesized a variety of reduced TiO_2 samples by using Zn powder as the reducing agent and HF as the solvent for the stabilization of the formed Ti^{3+} species and oxygen vacancies in a simple one-pot hydrothermal process. At the same time, it should be noted that the Ti^{3+} introduced by Zn reduction is not stable and is likely to be oxidized in air [28].

5.3. Electrochemical reduction synthesis

Zhang et al. demonstrated that that electrochemical reduction method is a facile and effective strategy to induce *in situ* self-doping of Ti^{3+} into TiO_2 and the self-doped TiO_2 photoelectrodes showed remarkably improved and very stable water splitting performance [30]. The hierarchical TiO_2 NTs were fabricated by a two-step anodization process. In the first step of anodization, the as-prepared Ti sheet as an anode was anodized at 60 V for 30 min in electrolytes consisted of 0.5 wt% NH_4F in EG solution with 2 vol% water and a Pt mesh (Aldrich, 100 mesh) as a cathode, respectively. After the as-grown nanotube layer was ultrasonically removed in DI water, the second step of anodization was performed at 80 V for 5 min. Then, the prepared TiO_2 NT samples were cleaned and annealed in air at 450 degree for 1 h with a heating rate of 5 degree min^{-1} [30]. In the electrochemical reduction processes, the TiO_2 NTs as the working electrode with an AgCl electrode and a Pt mesh formed a typical three-electrode system under a negative potential (0.4 V vs. the reversible hydrogen electrode (RHE)) in the supporting electrolyte of 1 M Na_2SO_4 for 30 min [30]. The electronic transition from the valence band to the Ti^{3+} induced interbands and/or from the energy band levels to the conduction band was considered to contribute to enhance the absorption in the visible region in the self-doped TiO_2, which helps explaining the observed color change from the prime white of the TiO_2 NTs to the light blue of the ECR-TiO_2 NTs [30].

5.4. Metal reduction method

Zheng et al. proposed an approach to synthesize blue TiO_2 nanoparticles with abundant oxygen deficiencies/Ti^{3+} species through Al reduction of TiO_2 nanosheets at 500°C [31]. Zhang et al. developed a reduction method to synthesize a series of TiO_{2-x} samples with their color changing from white to dark blue, which possess a much higher surface area and visible light absorption compared to pristine TiO_2 (**Figure 8**) [32]. In a typical reduction process, crystalline

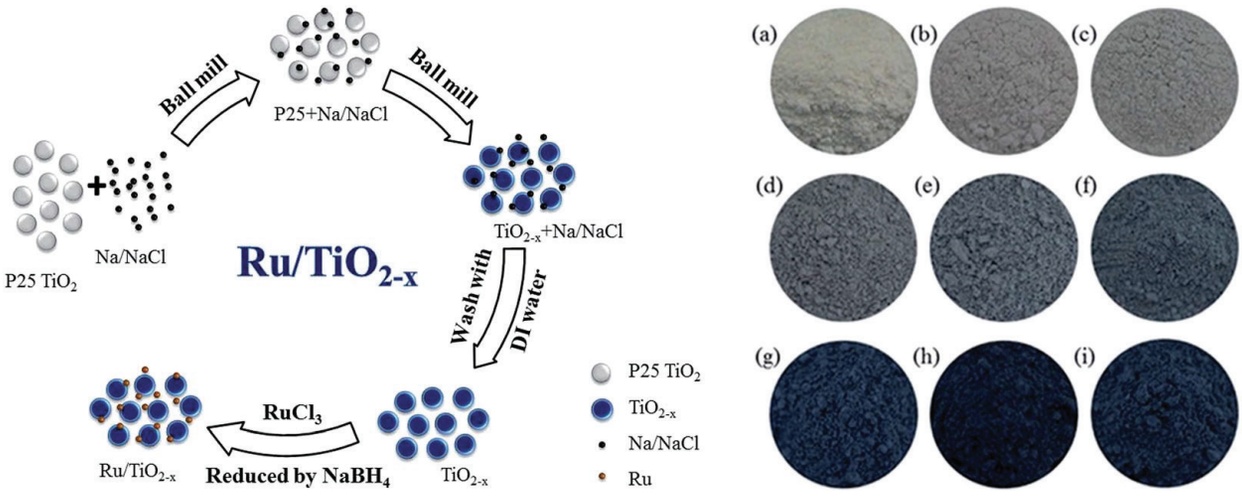

Figure 8. The route for the preparation of Ru/TiO_{2-x}; photographs of P_{25} nanocrystals and TiO_{2x}. (a) P_{25} nanocrystals, (b) TiO-1-80-0.5, (c) TiO-1-80-1, (d) TiO-1-120-4, (e) TiO-1-150-4, (f) TiO-1-180-4, (g) TiO-2-180-4, (h) TiO-3-180-4, and (i) TiO-4-180-4. Reprinted with permission from [32]. Copyright (2017) The Royal Society of Chemistry.

TiO_2 was milled with Na/NaCl fine powders with different weight ratio at a series of milling rates such as 80, 120, 150, and 180 rpm at room temperature under argon atmosphere for 0.25–4 h. After the Na and NaCl was removed, the obtained TiO_{2-x} products were dispersed in a small amount of deionized water and then vacuum-dried at room temperature to obtain TiO_{2-x} powders [32]. Moreover, the obtained TiO_{2-x} with a high surface area can be employed as an effective support for Ru particles and the Ru/TiO_{2-x} catalyst exhibited superior activity in the catalytic hydrogenation of N-methylpyrrole [32].

5.5. Phase-selective room-temperature solution processing

Until now, numerous methods to prepare blue TiO_2 have been reported, but all of them require high-temperature processing. Due to high-temperature processing, a phase-selective reduction between the anatase and rutile TiO_2 phases is almost impossible. For the first time, phase-selective "disorder engineered" Degussa P_{25} TiO_2 nanoparticles using simple room temperature solution processing was demonstrated as a very effective method to prepare modulatory TiO_2 [9]. The blue-colored TiO_2 nanoparticles were obtained by using a strong reducing agent consists of lithium in ethylenediamine (Li-EDA), which can disorder only the white rutile phase of P_{25}, while well maintaining white anatase TiO_2 [9]. Firstly, 14 mg metallic Li foil was dissolved in 20 ml ethanediamine to form a 1 mmol/ml solvated electron solution. Two hundred milligram of Degussa P_{25} (anatase, size: ~25 nm, rutile, size: ~140 nm, P25, size: 20–40 nm) was prepared after thorough drying and then added into the abovementioned solution and stirred for several days depending on the application. After sufficient reaction, the excess electrons and formed Li salts were quenched by slowly adding HCl into the mixture. Finally, the blue-colored TiO_2 nanoparticles were thoroughly rinsed by deionized water several times and dried at room temperature in a vacuum oven [9].

In their study, the blue TiO_2 showed drastically enhanced visible and near-infrared light absorption by induced abundant order/disorder junctions at the surface from selective disorder engineering, which means that it has well charge separation efficiency through type-II bandgap alignment and can effectively promote strong hydrogen evolution surface reaction [9]. Therefore, when the phase-selective disorder engineering of P_{25} TiO_2 nanoparticles as photocatalysts were used, they exhibited high stability and a high hydrogen evolution rate of 13.89 mmol h^{-1} g^{-1} using 0.5 wt% Pt (cocatalyst) and 3.46 mmol h^{-1} g^{-1} without using any cocatalyst under simulated solar light (**Figure 9**) [9].

5.6. Other methods

5.6.1. Sol-gelation hydrothermal technique and subsequent reduction treatment method

Ti^{3+} self-doped blue TiO_2 (B) single-crystalline nanorods (b-TR) were synthesized *via* three steps, in which the titanium dioxide powder was prepared via the sol-gelation approach followed by hydrothermal treatment. Blue TiO_2 (B) single-crystalline nanorods were obtained by further annealing at 350°C in Ar [33]. Under visible light illumination, the degradation rate of RhB reached 97.01% by b-TR and the photocatalytic hydrogen evolution rate was as high as 149.2 μmol h^{-1} g^{-1} under AM 1.5 irradiation [33]. The mechanistic

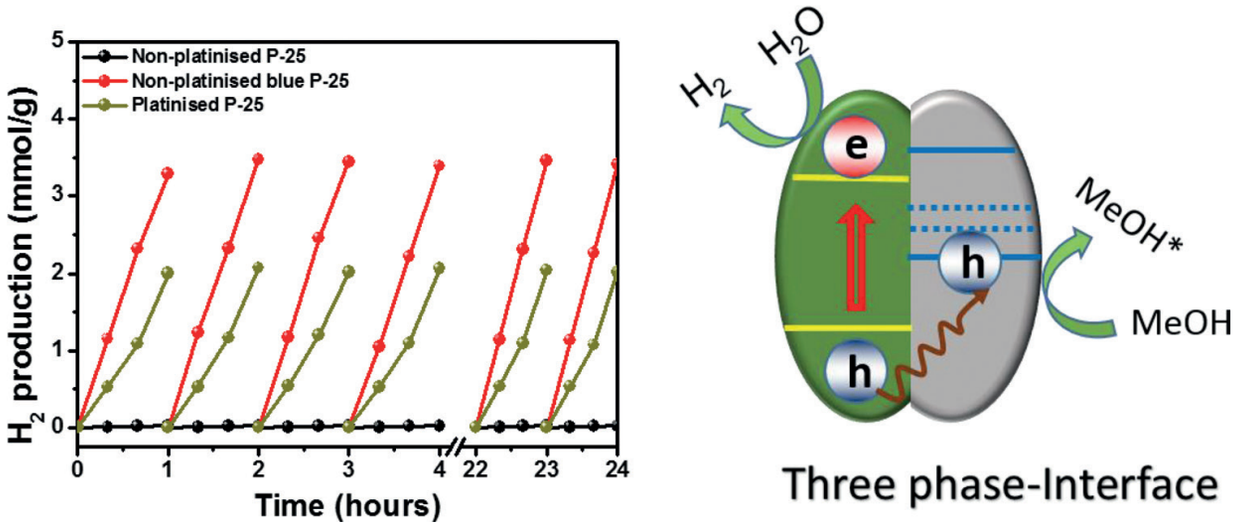

Figure 9. (a) Comparison of the hydrogen generation and cycling performance of 0.5 wt% platinized P_{25}, nonplatinized P_{25} and nonplatinized blue P_{25} after 1 day of continuous reaction using methanol as a sacrificial agent. A simulated full solar spectrum was used as the excitation source, which produced approximately 100 mW cm^{-2} in the samples, which consisted of various TiO_2 nanocrystals in a 100 mL quartz reactor filled with 70 mL of solution. (b) Proposed mechanism for charge separation and H_2 generation in blue P_{25} (green part: ordered TiO_2, gray part: disordered TiO_2). Copyright (2016), Royal Society of Chemistry [9].

analysis and characterization results showed that the synergetic action of the special TiO_2 (B) phase, Ti^{3+} self-doping, and the 1D rod-shaped single-crystalline nanostructure resulted in a narrowed bandgap of 2.61 eV, which enhanced the photocatalytic and photoelectrochemical performances [33] (**Figure 10**).

5.6.2. Ice-water quenching

Liu et al. applied ice-water quenching as a facile strategy for the synthesis of blue color of Ti^{3+} self-doped TiO_2 [23]. In the typical process, commercial P_{25} materials were quenched in

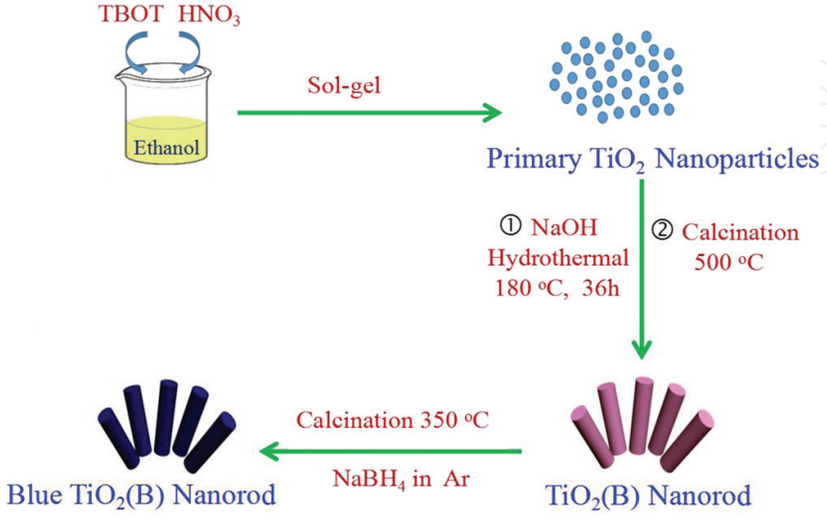

Figure 10. Diagrammatic sketch for the formation of blue TiO_2 (B) single-crystalline nanorod. Copyright (2016) American Chemical Society [33].

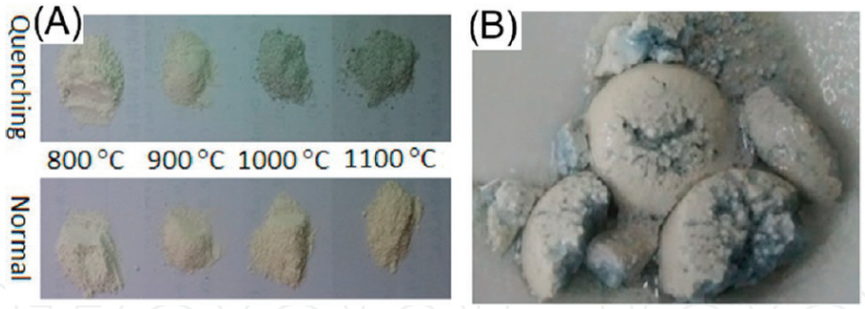

Figure 11. (A) Digital pictures of q-TiO_2 and n-TiO_2 samples prepared from the commercial P_{25} powders after being subjected to pre-annealing at different temperatures. (B) Digital picture of just-quenched TiO_2 sample on filter paper, which shows the blue color in the inner side of the sample [23]. Copyright (2017) American Chemical Society.

ice-water after pre-annealing at a high temperature. Then, the obtained powders were filtered and dried at 80°C for 12 h for further use [23]. Digital pictures of q-TiO_2 (quenched TiO_2) show that the color changed to pale blue when subjected to a temperature higher than 900°C, which confirmed the presence of Ti^{3+} in TiO_2 after ice-water quenching (**Figure 11**), implying that the d-d might be a transition from Ti^{3+} band gap states to their resonant excited states and extended light absorption together with near-IR absorption [23]. In addition, the surface distortion and the associated oxygen defects were considered to be contributed to the substantially enhanced photocatalytic activity [23]. It should be pointed out that the quenched TiO_2 cannot absorb much visible light, which means that the photoexcited electrons at the Ti^{3+} defect level cannot transfer outside [23].

6. Conclusions and development

In this chapter, blue TiO_2 that has a low energy bandgap is introduced as an advanced semiconducting material for possible applications in the visible-light-driven photocatalysis. A variety of preparation methods for blue TiO_2 photocatalysts with Ti^{3+} states of a high oxygen defect density have been successfully introduced. For the synthesis of the blue TiO_2 in the applications of photocatalysis, hydrogenation method using TiO_2 with hydrogen at 500°C or with hydride reducing agent at 450°C, hydrothermal method using Ti precursors or Zn powder reducing agent under HF solvent, electrochemical reduction method using anodizing TiO_2 at 60 and 80 V and then annealing at 450°C, and metal reduction method using Al at 500°C, Na and NaCl solid milling, or Li-EDA solution at room temperature and atmospheric pressure. For the preparation of blue TiO_2, the most recently developed metal solution room temperature method can give phase-selective reduction between the anatase and rutile TiO_2 phases. For the first time, the phase selective "disordered rutile and crystalline anatase" P_{25} TiO_2 nanoparticles are reported, which turns out that it is a very effective photocatalyst for hydrogen evolution reaction and removal of algae under solar irradiation. However, how to quantitatively control surface defects and the properties of the interface between the order and disorder surface layer still remain as important challenges to understand the true physicochemical properties of blue TiO_2.

As mentioned in the introduction, in the near future, we would like to further address beneficial applications in clean energy conversion and storage media and protecting the environment, including the hydrogen evolution reaction, carbon dioxide reduction, and degradation of pollutants by using noble blue TiO_2 under visible light.

Acknowledgements

This work was supported by IBS-R011-D.

Author details

Jianmin Yu[1,3†], Chau Thi Kim Nguyen[1,3†] and Hyoyoung Lee[1,2,3,4*]

*Address all correspondence to: hyoyoung@skku.edu

1 IBS Center for Integrated Nanostructure Physics, Institute for Basic Science (IBS), Sungkyunkwan University, Suwon, Republic of Korea

2 Department of Energy Science, Sungkyunkwan University, Suwon, Republic of Korea

3 Department of Chemistry, Sungkyunkwan University, Suwon, Republic of Korea

4 SKKU Advanced Institute of Nano Technology (SAINT), Sungkyunkwan University, Suwon, Republic of Korea

† These authors contributed equally to the work.

References

[1] Gupta SM, Tripathi M. A review of TiO_2 nanoparticles. Chinese Science Bulletin. 2011; **56**(16):1639-1657

[2] Fujishima A, Honda K. Electrochemical photolysis of water at a semiconductor electrode. Nature. 1972;**238**:37

[3] Banerjee B et al. Green synthesis of Pt-doped TiO_2 nanocrystals with exposed (001) facets and mesoscopic void space for photo-splitting of water under solar irradiation. Nanoscale. 2015;**7**(23):10504-10512

[4] Buso D et al. Gold-nanoparticle-doped TiO_2 semiconductor thin films: Optical characterization. Advanced Functional Materials. 2007;**17**(3):347-354

[5] Hu Y, Tsai H-L, Huangk C-L. Effect of brookite phase on the anatase–rutile transition in titania nanoparticles. Journal of the European Ceramic Society. 2003;**23**:691-696

[6] Mor GK et al. A review on highly ordered, vertically oriented TiO_2 nanotube arrays: Fabrication, material properties, and solar energy applications. Solar Energy Materials and Solar Cells. 2006;**90**(14):2011-2075

[7] Qiu J. Hydrogenation synthesis of blue TiO_2 for high-performance lithiumion batteries. Journal of Physical Chemistry C. 2014;**118**:8824−8830

[8] Khader MM, Kheiri FMN, El-Anadouli BE, Ateya BG. Mechanism of reduction of rutile with hydrogen. The Journal of Physical Chemistry. 1993;**97**:6074−6077

[9] Zhang K et al. An order/disorder/water junction system for highly efficient co-catalyst-free photocatalytic hydrogen generation. Energy & Environmental Science. 2016;**9**(2):499-503

[10] Qiu J et al. Hydrogenation synthesis of blue TiO_2 for high-performance lithium-ion batteries. The Journal of Physical Chemistry C. 2014;**118**(17):8824-8830

[11] Pan J, Liu G, (Max) Lu GQ, Cheng H-M. On the true photoreactivity order of {001}, {010} and {101} facets of anatase TiO_2 crystals. Angewandte Chemie-International Edition. 2011;**50**(9): 2133-2137

[12] Gordon TR et al. Nonaqueous synthesis of TiO_2 nanocrystals using TiF_4 to engineer morphology, oxygen vacancy concentration, and photocatalytic activity. Journal of the American Chemical Society. 2012;**134**(15):6751-6761

[13] Liu X, Bi Y. In situ preparation of oxygen-deficient TiO_2 microspheres with modified {001} facets for enhanced photocatalytic activity. RSC Advances. 2017;**7**(16):9902-9907

[14] Cushing SK et al. Effects of defects on photocatalytic activity of hydrogen-treated titanium oxide nanobelts. ACS Catalysis. 2017;**7**(3):1742-1748

[15] Ola O, Maroto-Valer MM. Review of material design and reactor engineering on TiO_2 photocatalysis for CO_2 reduction. Journal of Photochemistry and Photobiology C: Photochemistry Reviews. 2015;**24**:16-42

[16] Indrakanti VP, Kubicki JD, Schobert HH. Photoinduced activation of CO_2 on Ti-based heterogeneous catalysts: Current state, chemical physics-based insights and outlook. Energy & Environmental Science. 2009;**2**(7):745

[17] Ishchenko OM. Semiconductor photocatalysis: Materials, mechanisms and applications. In: Caodoi W. editor. Chapter 2, Influences of Doping on Photocatalytic Properties of TiO_2 Photocatalyst. DOI: 10.5772/62774

[18] Kim Y et al. Solar-light photocatalytic disinfection using crystalline/amorphous low energy bandgap reduced TiO_2. Scientific Reports. 2016;**6**:25212

[19] Diebold U. The surface science of titanium dioxide. Surface Science Reports. 2003;**48**: 53-229

[20] Zhu G et al. Hydrogenated blue titania with high solar absorption and greatly improved photocatalysis. Nanoscale. 2016;**8**(8):4705-4712

[21] Su J, Zou X, Chen J-S. Self-modification of titanium dioxide materials by Ti^{3+} and/or oxygen vacancies: New insights into defect chemistry of metal oxides. RSC Advances. 2014;**4**(27):13979-13988

[22] Yu X, Kim B, Kim YK. Highly enhanced photoactivity of anatase TiO_2 nanocrystals by controlled hydrogenation-induced surface defects. ACS Catalysis. 2013;**3**(11):2479-2486

[23] Li JJ et al. Efficient promotion of charge transfer and separation in hydrogenated TiO_2/WO_3 with rich surface-oxygen-vacancies for photodecomposition of gaseous toluene. Journal of Hazardous Materials. 2018;**342**:661-669

[24] Liu B et al. Ice-water quenching induced Ti^{3+} self-doped TiO_2 with surface lattice distortion and the increased photocatalytic activity. The Journal of Physical Chemistry C. 2017;**121**(36):19836-19848

[25] Samsudin EM et al. Surface modification of mixed-phase hydrogenated TiO_2 and corresponding photocatalytic response. Applied Surface Science. 2015;**359**:883-896

[26] Wang W et al. A new sight on hydrogenation of F and N-F doped {001} facets dominated anatase TiO_2 for efficient visible light photocatalyst. Applied Catalysis B: Environmental. 2012;**127**:28-35

[27] Sun L et al. Design and mechanism of core-shell TiO_2 nanoparticles as a high-performance photothermal agent. Nanoscale. 2017;**9**(42):16183-16192

[28] Fang W et al. Zn-assisted TiO_{2-x} photocatalyst with efficient charge separation for enhanced Photocatalytic activities. The Journal of Physical Chemistry C. 2017;**121**(32):17068-17076

[29] Zhu Q et al. Stable blue TiO_{2-x} nanoparticles for efficient visible light photocatalysts. Journal of Materials Chemistry A. 2014;**2**(12):4429

[30] Zhang Z et al. Electrochemical reduction induced self-doping of Ti^{3+} for efficient water splitting performance on TiO_2 based photoelectrodes. Physical Chemistry Chemical Physics. 2013;**15**(37):15637-15644

[31] Zheng J et al. Facile aluminum reduction synthesis of blue TiO_2 with oxygen deficiency for lithium-ion batteries. Chemistry. 2015;**21**(50):18309-18315

[32] Zhang M et al. Room temperature synthesis of reduced TiO_2 and its application as a support for catalytic hydrogenation. RSC Advances. 2017;**7**(8):4306-4311

[33] Zhang Y et al. Ti^{3+} self-doped blue TiO_2(B) single-crystalline Nanorods for efficient solar-driven Photocatalytic performance. ACS Applied Materials & Interfaces. 2016;**8**(40): 26851-26859